BOUNDARY LAYER SEPARATION CONTROL USING A STEP-WALL CONICAL DIFFUSER WITH AN ANNULAR INLET

Kin Pong Lo
Department of Mechanical Engineering
Stanford University
488 Escondido Mall, Building 500 Room 501W, Stanford, CA 94305
kplo@stanford.edu

Christopher J. Elkins
Department of Mechanical Engineering
Stanford University
488 Escondido Mall, Building 500 Room 500K, Stanford, CA 94305
celkins@stanford.edu

John K. Eaton
Department of Mechanical Engineering
Stanford University
488 Escondido Mall, Building 500 Room 501F, Stanford, CA 94305
eatonj@stanford.edu

ABSTRACT

Practical applications of conical diffusers often involve an upstream annular flow passage created by a center body that is present for structural or other design requirements. The wake of the center body can cause the diffuser wall boundary layer to separate in an unpredictable manner. Flow separation can degrade the diffuser performance and fatigue downstream components and therefore must be controlled. A step-wall diffuser can be used to control the wall separation by fixing its location. The present experiment utilizes magnetic resonance velocimetry to acquire three-component mean velocity measurements for a set of step-wall conical diffusers with an annular inlet. The results show that the step separation bubble is predictable and stable. Reduction in the overall diffuser length is achieved by using three-dimensional perturbations to shorten the reattachment length of the step separation bubble.

INTRODUCTION

Conical diffusers are common in engineering design when the flow velocity needs to be decreased and the static pressure needs to be increased. For example, in a combined cycle power plant, the diffuser between the power turbine and the steam generator fulfills such requirements. The function of the diffuser is to lower the outlet pressure for the last stage turbine and reduce the inlet velocity for the steam generator. Flow separation is inevitable in a large area ratio diffuser because of the sustained adverse pressure gradient. The presence of flow separation is disadvantageous because it reduces the pressure recovery of the diffuser. Flow stability and uniformity also suffer, causing detrimental effects on downstream components. In the power plant example, the boiler effectiveness will be reduced by a non-uniform flow while the components will be fatigued by an unstable flow.

Flow in conical diffusers has been an active research topic in the past decades. Sovran and Klomp (1967), Klein (1981), and Azad (1996) reviewed numerous experiments on conical diffusers with circular inlets. However, practical applications of conical diffusers often involve an annular inlet instead. In the power plant example, the bearing hub of the turbine acts as a center body that forms an annular passage upstream of the diffuser.

The center body of the annular inlet creates a wake that can significantly affect the flow downstream in the diffuser. Our previous work (Lo et al. 2011) showed specifically that the boundary layer development along the diffuser outer wall is highly dependent on the flow in the center region. In the presence of an adverse pressure gradient, the separated wake of the center body extends over the entire diffuser length. The blockage effect of this separation bubble relieves the adverse pressure gradient and results in a relatively thin boundary layer along the outer diffuser wall. This central separation bubble can be dramatically shortened by using Coanda blowing to entrain high momentum main flow

toward the center. However, this results in a slow and thick boundary layer along the outer wall. In cases where Coanda blowing is too strong, the boundary layer separates and results in reverse flow along the diffuser wall. Although the conical diffuser is axisymmetric, the boundary layer does not separate all around the circumference of the outer wall. The onset of boundary layer separation occurs at an unpredictable location on the outer wall. Furthermore, the separation could change due to minor variations in the inlet conditions. Moreover, once the boundary layer separates, it does not reattach before the end of the diffuser. Therefore, the outer wall boundary layer separation must be controlled.

A backward-facing step has a well-defined separation bubble behind the step. The flow separates at the edge across the span of the step and reattaches downstream. It is possible to incorporate a backward-facing step into the diffuser wall, as shown in Figure 1a. This configuration forces the flow to separate all around the circumference of the outer wall behind the step. In other words, the wall boundary layer separation is made predictable, and its location is fixed. However, it is unclear how the step separation bubble will interact with the center body wake, both with and without Coanda blowing, and consequently affect the flow in the diffuser downstream. Another advantage of using a step-wall diffuser is the reduction of the overall diffuser length, which is achieved by shortening the step length. However, a robust mechanism must first be used to shorten the reattachment length before the step length can be reduced. Park et al. (2007) have shown that using three-dimensional perturbations to induce longitudinal vortices can reduce the reattachment length. These vortices enhance mixing across the shear layer that bounds the separation bubble. It is, however, unclear if this mechanism will work in a circular flow passage. Also, this shear layer interacts with the wake of the center body and affects the boundary layer development downstream. The effect of this complex interaction is unknown.

The present paper examines the use of a step-wall conical diffuser to control the diffuser outer wall boundary layer separation. Achievable reduction of the overall diffuser length has also been investigated. Velocity fields in a number of diffuser models are measured using magnetic resonance velocimetry (MRV). Three-component mean velocity data are obtained in a three-dimensional grid. The diffuser models mimic the key geometry of the back diffuser in a combined cycle power generation plant.

EXPERIMENTAL SETUP

The MRV experiments were performed at the Richard M. Lucas Center for Imaging, using a General Electric 1.5T model S3 whole body scanner. Three-component velocity measurements were obtained on a uniform Cartesian mesh following the phase contrast MRV techniques described by Elkins et al. (2003). The velocity encoding (VENC) values control the maximum measurable velocity that will be free of aliasing. The VENC values were 5 m/s for all three directions for the main experiments. A flip angle of 15 degrees was used. The X-axis is the streamwise direction, while the Y- and Z-axes are the vertical and spanwise directions, respectively. The XZ plane field of view has a nominal dimension of 280 mm by 280 mm, and an effective dimension of 280 mm by 126 mm due to a phase FOV factor of 0.45. The spatial resolution in the X, Y, and Z directions are 1.09 mm, 1 mm, and 1.09 mm, respectively. The velocity data are measured on a uniform grid with 256 points in the X direction, 106 points in the Y direction, and 116 points in the Z direction.

Figure 1a shows a smooth edge step-wall diffuser model configuration. It consists of similar hardware as the one used by Lo et al. (2011). Not shown in the figure is the inlet section, which is designed to produce a nearly uniform flow at the diffuser inlet. It is made up of a conical diffuser with two turbulence grids to prevent boundary layer separation, followed by a 560 mm long by 76 mm ID acrylic pipe. A 1.6:1 area ratio contraction is used to reduce the flow passage diameter to match the OD of the annular inlet for the diffuser test section. Following the inlet section is a center body section, which forms an annular inlet to the diffuser downstream. The center body is a cylinder with a bullet nose in the front. The nose has an elliptic profile with a minor axis of 16.6 mm and a major axis of 50 mm. The center body has a diameter of D_{cb}=33.3 mm, and a length of 105 mm. A 1.6 mm high boundary layer trip is located on the center body surface to create a turbulent boundary layer along the surface. Five hollow struts support the center body from the OD of the annulus, which is 60.7 mm. The struts are shaped with a truncated NACA 0024 airfoil profile. The annulus OD starts expanding at 75 mm downstream of the center body nose to an OD of 66.5 mm at the end of the center body section.

All experiments described here had a Coanda tail piece attached to the base of the center body. In some cases the flow to the Coanda jet was turned off. In that case, the blowing ratio defined as the bulk average velocity at the jet exit, divided by the average velocity in the annulus upstream of the struts (U_{bulk}) was BR=0. In other cases where the Coanda jet was turned on, fluid was supplied to an annular plenum inside the center body through the five hollow struts. A curved wall jet is formed at the exit by accelerating the fluid through the flow passage inside the Coanda tail piece. The jet exit height is 0.7 mm and the outer lip is 0.5 mm thick. The lip is supported by five struts that take the shape of a truncated NACA 0020 airfoil. The Coanda tail piece is 26.4 mm long and has an elliptic back end with a minor axis of 15.4 mm and a major axis of 16.4 mm.

A straight section with a constant diameter of 66.5 mm and a length of one diameter is attached to the end of the center body section. The end of the straight section can be modified to incorporate a wavy edge, as shown in Figure 1b, in order to perturb the flow. The wavy edge has a sinusoidal profile with twelve periods and a peak-to-trough value of 3.5 mm. The total length of the straight section, which now includes the perturbation section, remains unchanged. Downstream of the straight section is a step-wall conical

diffuser, which consists of a constant diameter step section followed by an expanding section. The diameter of the step section is D_i=80.5 mm, which results in an axisymmetric step with step height h=7 mm when it is connected to the straight section. The length of the step section is the step length *l*, which can be changed by using a different step section. The outlet diameter of the expanding section is D_o=94.6 mm. The expanding section has a half angle of 6 degrees. An exit plenum is attached to the diffuser exit and allows plumbing connections to be made using PVC tubing.

Water is used as the working fluid and is circulated in a closed loop system. In order to improve signal quality, copper sulfate is added to the water at a concentration of 0.06 molar. Two Berkeley BPDH10-L electric pumps are used to drive the main flow, while a Little Giant TE-6-MD-HC electric pump is used to drive the Coanda jet flow. The volume flow rate of the main flow is measured by a Signet Instruments 8550 Flow Transmitter connected to a 515 Paddlewheel Flow Sensor. The Coanda jet volume flow rate is measured using a Blue-White Industries F-1000-RB flow meter.

All velocity measurements presented below are normalized by U_{bulk}, which was set to approximately 2.3 m/s. The Reynolds number Re_{Dh} based on U_{bulk} and the hydraulic diameter D_h of the annulus is between 61000 and 64000 for all the experiments described here.

An estimate of the velocity measurement uncertainty is calculated to be 0.07 m/s or 3% of U_{bulk} at 95% confidence level, as described by Elkins et al. (2003).

RESULTS AND DISCUSSIONS

The present study focuses on controlling the outer wall boundary layer separation using various step-wall diffusers. The first step-wall diffuser had an axisymmetric step with a step length *l*=9.5h. This configuration was tested with the Coanda tail piece in place but no flow through the Coanda jet (BR=0). Contours of the streamwise velocity component U_x are shown in Figure 2. The contour values are azimuthally averaged and normalized by U_{bulk}. Azimuthally averaged velocity vectors are overlaid to visualize velocity profile development. A separation bubble is present in the immediate wake of the center body. The straight section defers the onset of the adverse pressure gradient and allows the central separation bubble to close without Coanda blowing. However, the flow still enters the diffuser with a strong velocity deficit at the center. The flow separates at the step edge and forms a recirculating region downstream of the step. When the total reverse flow area is less than 1% of the total flow area, the flow is considered to have reattached. Using this criterion, the flow reattaches at around 9.2h downstream of the step and the separation bubble is considered to be closed. The boundary layer grows along the outer wall but remains attached all the way to the diffuser exit. The center region of the flow remains slow throughout the diffuser as the adverse pressure gradient continues to decelerate the center body wake.

Coanda blowing is then turned on and set at BR=1.0 in order to eliminate the central separation bubble. The jet mass flow rate was 3.3% of the main flow rate. Figure 3 shows the contours of U_x/U_{bulk}. The wake of the center body has no reverse flow due to the strong entrainment of the Coanda jet, and the flow enters the diffuser with a relatively flat velocity profile. Again, the flow separates at the edge of the step and a recirculating region is formed. The reattachment length of the step separation bubble is around 8.4h. The boundary layer along the outer wall is thicker than the BR=0 case, but remains attached all the way to the diffuser exit.

When the Coanda blowing is increased to BR=1.3, a high velocity jet is formed in the wake of the center body, as shown by the U_x/U_{bulk} contours in Figure 4. The flow enters the diffuser and, again, separates at the edge of the step. The reattachment length is around 8.8h. The outer wall boundary layer is thicker than the BR=1.0 case, but still remains attached all the way to the diffuser exit. The adverse pressure gradient decelerates the jet at the center, and the velocity profile is relatively flat at the exit of the diffuser.

A previous experiment using a smooth-wall conical diffuser in the same apparatus showed that the outer wall boundary layer separates when Coanda blowing is set at BR=1.3. On the other hand, results from the present study show that the step separation bubble behaves similarly regardless of the strength of Coanda blowing for the range of blowing ratios tested. The reattachment length varies between 8.4h and 9.2h. This variation in the reattachment length is relatively insignificant due to inaccuracy of area measurement caused by partial volume effect and artifacts near a fluid/liquid boundary. The outer wall boundary layer remains attached for the three cases mentioned above. Therefore, using the step-wall diffuser is a robust way to stabilize the outer wall boundary layer separation.

The overall length of the diffuser can be reduced if the step separation bubble reattachment length, and consequently the step length, can be reduced. The key is to enhance mixing across the shear layer that bounds the step separation bubble. A three-dimensional geometric perturbation as shown in Figure 1b is used to induce longitudinal vortices, which are responsible for large scale mixing. Figures 5a and 5b show the contours of U_x/U_{bulk} azimuthally averaged among the troughs and peaks, respectively, for BR=0. The central separation bubble is slightly longer than the case without the perturbation section, due to the adverse pressure gradient imposed by the perturbation section, which has an increasing cross-sectional area. The flow enters the diffuser with a strong velocity deficit at the center and separates unevenly at the edge of the step. At the trough locations, the flow follows the troughs toward the outer wall. As a result, there is no measurable reverse flow downstream of the troughs. On the other hand, at the peak locations, recirculating regions are formed downstream of the peaks. However, the reattachment length of this separation bubble is around 4.7h, which is just over half of what it is without the perturbation section. Since the step length of 9.5h is more than twice the reattachment length, the flow near the step

wall downstream of the reattached shear layer can gain momentum before reaching the diffusing wall. Compared with the case without the perturbation section, the boundary layer along the diffuser wall is thinner and the center region of the flow is slightly slower at the diffuser exit.

Figures 6a and 6b show the contours of U_x/U_{bulk} azimuthally averaged among the troughs and peaks for the same geometry with BR=1.0. Again, there is no reverse flow in the immediate wake of the center body and the flow enters the diffuser with a relatively flat velocity profile. The flow separates unevenly at the edge of the step, similar to the BR=0 case with perturbation. There is no measurable recirculating region downstream of the troughs, and the separation bubbles downstream of the peaks have a reattachment length of 4.2h. The boundary layer along the diffuser wall is again faster than the BR=1.0 case without perturbation. These results show that, for the two blowing ratios tested, the wavy edge successfully reduces the reattachment length of the step separation bubble.

In order to understand the mechanism responsible for the reattachment length reduction, secondary flow structures downstream of the wavy edge must be resolved. Measurements were repeated for the wavy step configuration with BR=0 using lower VENC values to improve the velocity resolution for the secondary flow. Figure 7a shows the contours of U_x/U_{bulk} on a transverse plane 1h downstream of the step. The step separation bubble has a distinct peak-and-trough pattern, and the shear layer that bounds the bubble follows the shape of the wavy edge. Figure 7b shows a detailed view of the upper left corner of the plane. Secondary velocity vectors are projected onto the plane and overlaid to aid visualization of the secondary flow structures. A pair of counter-rotating longitudinal vortices is observed downstream of each peak. These vortex pairs have the opposite sense of a horseshoe vortex. They entrain fluid from the separation bubble to the main flow and carry fluid from the main flow to the recirculating regions. In other words, these vortices enhance mixing across the shear layer. They also interact with each other and their corresponding images due to the induced velocity. This results in large-scale fluid motion across the shear layer. It is the strong mixing and fluid motion that allow the separated shear layer to reattach quickly.

In an attempt to reduce the overall diffuser length, the step length *l* was shortened to 5h and tested at BR=1.0. Figures 8a and 8b show the contours of U_x/U_{bulk} azimuthally averaged among the troughs and peaks, respectively. The reattachment length is around 4.1h. The overall diffuser length is reduced by 23%. It is important to note that the center region of the flow is slower than the case with a 9.5h long step. In fact, the center region is so slow that the flow is reversed near the diffuser exit. This is due to a stronger radial velocity component in the flow, which is caused by the shortening of the step length. Near the reattachment point, the flow has a significant radial velocity toward the wall. When there is extra length between the reattachment point and the start of the diffusing wall, the flow has to realign itself with the main flow direction thus reducing the radial velocity component. On the other hand, when the wall expansion begins close to the reattachment point, the flow maintains a radial velocity component as it follows the diverging wall. As a result, there is a stronger mean radial flux of X momentum, which in turns slow down the center region. Another experiment where the same geometry was tested at BR=1.1 demonstrated an increase in the velocity in the center region and the elimination of the flow reversal at the diffuser exit.

The possibility of further reduction in the diffuser length has been explored by repeating the experiment with *l* reduced to 4h. Figures 9a and 9b show the contours of U_x/U_{bulk} azimuthally averaged among the troughs and peaks, respectively. The step separation bubble is not completely closed by the end of the step length, where around 3% of the flow area is reverse flow. These reverse flow regions extend beyond the step onto the diffuser outer wall. As a result, the boundary layer is very thick and has pockets of reversed flow. Therefore *l*=4h is too short and leads to unstable flow in the diffuser.

CONCLUSION

Three-component mean velocity field measurements were acquired for a set of conical diffusers with an annular inlet. The center body of the annular inlet creates a central separation bubble that extends over the entire diffuser length. Coanda blowing can mitigate this central separation, but at the same time the boundary layer along the diffuser wall becomes thick and in some cases separates in an unpredictable manner. A backward-facing step incorporated into the outer wall of the conical diffuser acts to stabilize the boundary layer separation. Results show that the behavior of the step separation bubble is predictable, stable, and independent of the Coanda blowing ratio.

A three-dimensional geometric perturbation at the step edge shortens the reattachment length of the step separation bubble by nearly a factor of two, and breaks the large axisymmetric step separation bubble into a set of much smaller bubbles. This would be expected to reduce large scale unsteadiness in the flow, although this has not been documented in the present experiment.

The reduction in reattachment length allows an overall reduction in the diffuser length. However, the mean radial flux of X momentum increases when the diffusing wall is near the reattachment point of the step separation bubble. This results in a slow center region and possible flow reversal at the exit of the diffuser. Stronger Coanda blowing is required to speed up the center region to prevent flow reversal.

ACKNOWLEDGEMENT

Funding for this research is provided by Siemens Energy. Dr. Matthew Montgomery of Siemens provided much useful input.

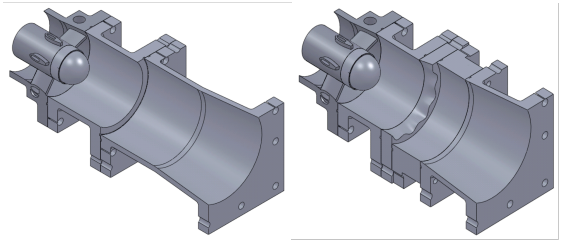

(a) (b)

Figure 1. (a) Smooth edge step-wall diffuser model, (b) wavy edge step-wall diffuser model.

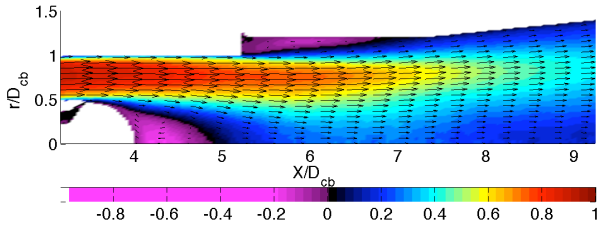

Figure 2. Azimuthally averaged streamwise velocity U_x/U_{bulk} contour plot with velocity vectors projection. Coanda blowing is turned off (BR=0). Smooth step with a step length *l*=9.5h.

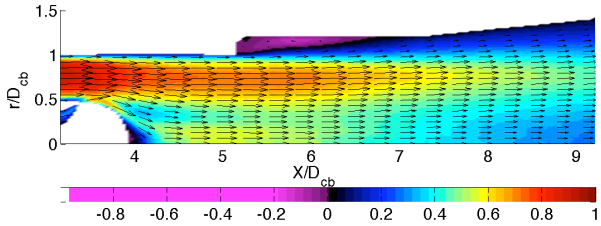

Figure 3. Azimuthally averaged streamwise velocity U_x/U_{bulk} contour plot with velocity vectors projection. Coanda blowing is turned on and set at BR=1.0. Smooth step with a step length *l*=9.5h.

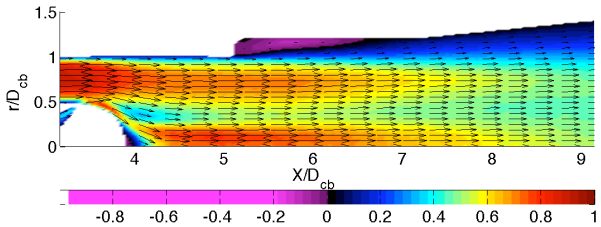

Figure 4. Azimuthally averaged streamwise velocity U_x/U_{bulk} contour plot with velocity vectors projection. Coanda blowing is turned on and set at BR=1.3. Smooth step with a step length *l*=9.5h.

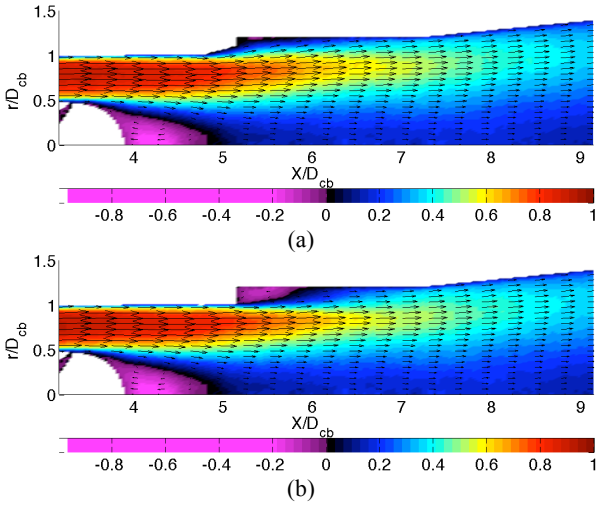

Figure 5. Azimuthally averaged streamwise velocity U_x/U_{bulk} contour plot with velocity vectors projection. (a) averaged among all troughs, (b) averaged among all peaks. Coanda blowing is turned off (BR=0). Wavy step with a step length *l*=9.5h.

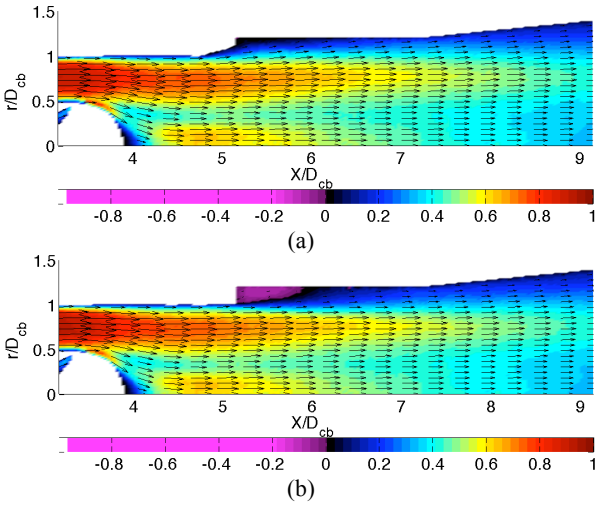

Figure 6. Azimuthally averaged streamwise velocity U_x/U_{bulk} contour plot with velocity vectors projection. (a) averaged among all troughs, (b) averaged among all peaks. Coanda blowing is turned on and set at BR=1.0. Wavy step with a step length *l*=9.5h.

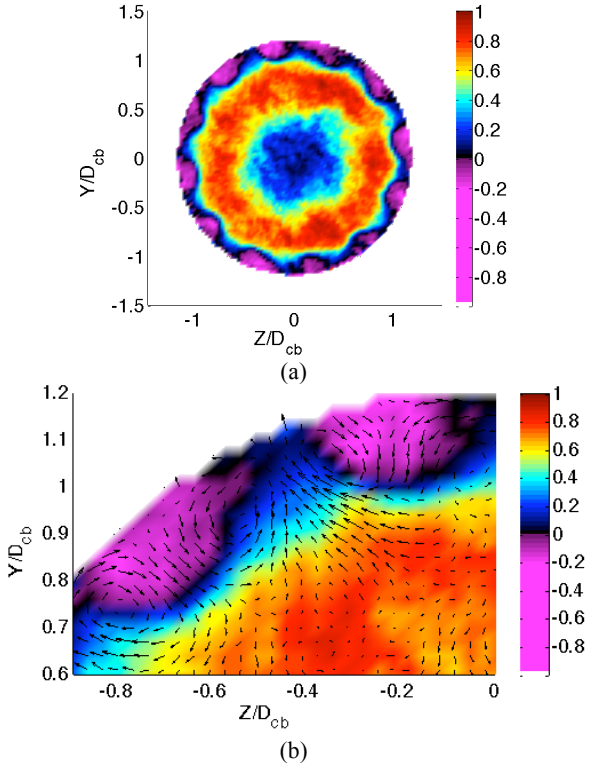

Figure 7. (a) Streamwise velocity U_x/U_{bulk} contour plot on a transverse plane located 1h downstream of the wavy step. Coanda blowing is turned off (BR=0). (b) Detail view of the upper left corner of (a) with velocity vectors projection overlaid.

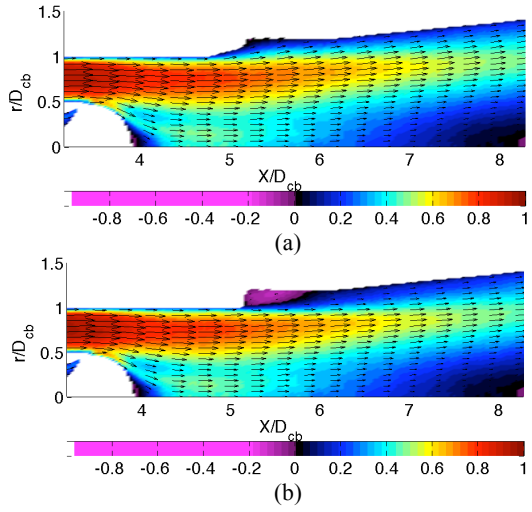

Figure 8. Azimuthally averaged streamwise velocity U_x/U_{bulk} contour plot with velocity vectors projection. (a) averaged among all troughs, (b) averaged among all peaks. Coanda blowing is turned on and set at BR=1.0. Wavy step with a step length *l*=5h.

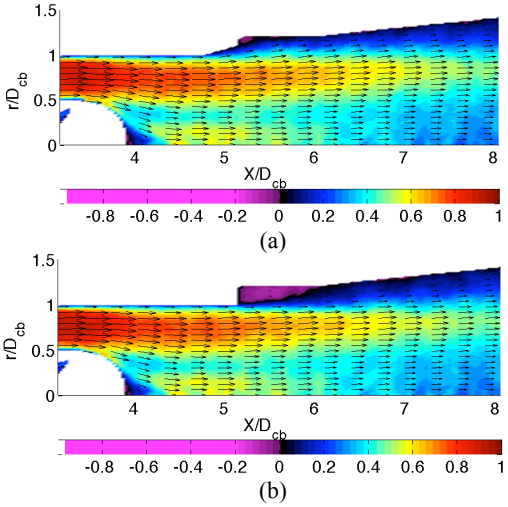

Figure 9. Azimuthally averaged streamwise velocity U_x/U_{bulk} contour plot with velocity vectors projection. (a) averaged among all troughs, (b) averaged among all peaks. Coanda blowing is turned on and set at BR=1.0. Wavy step with a step length *l*=4h.

REFERENCES

Azad, R. S., 1996, "Turbulent Flow in a Conical Diffuser: A Review", *Experimental Thermal and Fluid Science*, 13:318-337.

Elkins, C. J., Markl, M., Pelc, N., Eaton, J. K., 2003, "4D magnetic resonance velocimetry for mean velocity measurements in complex turbulent flows", *Exp. Fluids*, 34(4):494-503.

Klein, A., 1981, "Review: Effects of Inlet Conditions on Conical-Diffuser Performance", *Journal of Fluids Engineering*, 103, pp. 250-257.

Lo, K. P., Elkins, C. J., Eaton, J. K., 2011, "Separation Control in a Conical Diffuser with Annular Inlet: Center Body Wake Separation".

Park, H., Jeon, W. P., Choi, H., Yoo, J. Y., 2007, "Mixing enhancement behind a backward-facing step using tabs", *Physics of Fluids*, 19, 105103.

Sovran, G., and Klomp, E. D., 1967, "Experimentally Determined Optimum Geometries for Rectilinear Diffusers with Rectangular, Conical or Annular Cross-Section", *Fluid Mechanics of Internal Flow*, pp. 270-319.